doi.org/10.36721/PJPS.2021.34.5.SUP.1923-1928.1

Combination of eudragit EPO with poloxamers for improved solubility and dissolution of Zafirlukast: An evaluation of solid dispersion formulations

Zeeshan Masood*, Muhammad Tayyab Ansari and Samina Afzal
Department of Pharmaceutical Chemistry, Faculty of Pharmacy, Bahauddin Zakariya University, Multan, Pakistan

Abstract: This study investigated the effect of solid dispersions (SD) on solubility and release of Zafirlukast (ZA) by physical mixture (PM), solvent evaporation (SE) and kneading method (KM) with Eudragit EPO (EPO) as binary component and Poloxamer 188 (P188) and Poloxamer 407 (P407) as ternary components. The binary and ternary systems caused an increase of 322 folds and 356 folds in aqueous solubility of ZA, respectively. Formulations were characterized for solubility, FTIR, PXRD, DSC, SEM and dissolution studies. P407 was found to be an excellent solubility booster in combination with EPO. It was concluded that solubility and dissolution rate of ZA increased significantly when SD of the ZA was prepared by solvent evaporation method (1:7 ratio) using 15% P407 as ternary component.

Keywords: Zafirlukast, solubility, solvent evaporation, solid dispersions.

INTRODUCTION

Zafirlukast (ZA) is chemically an indole nucleus containing diarylmethane as cyclopentyl N-[3-[[2-methoxy-4[(2-methylphenyl) sulfonylcarbamoyl] phenyl] methyl]-1methylindol-5-yl]carbamate (Rajasekhar *et al.*, 2016, Yang *et al.*, 2020). It is a selective cysteinyl leukotriene-1 receptor antagonist that is given orally for the treatment of asthmatic conditions (Schierle *et al.*, 2018). In recent developments, Zafirlukast has been identified as excellent drug repositioning agent for COVID-19 as a novel and promising pharmacotherapeutic agent in this pandemic tenure (Delijewski and Haneczok, 2021). Further clinical reports reveal that it exerts a wide range of effects including preventive effect on ox-LDL-induced formation of foam cells in arterial disease (Song *et al.*, 2020), protects blood-brain barrier integrity from ischemic brain injury (Zeng *et al.*, 2020), antineoplastic properties against hepatocellular carcinoma via activation of mitochondrial mediated apoptosis (Kumar *et al.*, 2019), anti-asthmatic, anti-inflammatory and oral anti-bacterial activities (Lei *et al.*, 2019). It is poorly aqueous soluble (BCS II class), possesses low oral bioavailability leading to limited and slow release pattern in body fluids (Barkat *et al.*, 2019, McPherson *et al.*, 2020)

Eudragit EPO (EPO) is a basic butylated methacrylate cationic copolymer based on dimethytaminoethyl methacrylate, butyl methacrylate and methyl methacrylate in a ratio 2:1:1. It is soluble in gastric fluid up to pH 5 which can facilitate higher drug solubilization in the acidic medium (Drašković *et al.*, 2017, Porfiryeva *et al.*, 2019) It is extensively used as solubilizing agent, mucoadhesive and taste masking agent (Lin *et al*., 2018)

**Corresponding author:* e-mail: zmpharma@gmail.com

Poloxamer 188 (P188) and poloxamer 407 (P407) are nonionic polyoxyethylene-polyoxypropylene copolymers used in pharmaceutical formulations as solubilizing, stabilizing and wetting agents (Agafonov *et al.*, 2019, Nanaki *et al.*, 2019, Tambe and Pandita, 2018).

The present study was an attempt to identify the effect of binary solid dispersion of EPO with ZA and P188 and P407 based ternary solid dispersions for the improvement of ZA's aqueous solubility and oral bioavailability by the application of physical mixture (PM), solvent evaporation (SE) and kneading method (KM).

MATERIALS AND METHODS

ZA was purchased from Beijing Mesochem Technology Co., Ltd. China. The P188 and P407 were purchased from Sigma. EPO was gifted from Evonik, Germany. All other chemicals were of analytical or HPLC grade.

Preparation of binary and ternary SDs

ZA and carrier polymers binary and ternary SD were prepared at various ratios of Eudragit EPO and poloxamers 188 and 407 as shown in table 1. SDs by PM were prepared by gently mixing and triturating material for an hour, which were then dried in oven at 37^{o}C. In order to prepare SDs by SE, ZA was dissolved in acetone whereas EPO, P188 and P407 were dissolved in methanol separately followed by mixing the solvents and then evaporating the resultant mixture in a vacuum oven at 40^{o}C for 48 hours. For KM based SDs, ZA and polymers were triturated in a mortar with small volumes of solvent blend of acetone: Methanol. The thick slurries were kneaded for 45 minutes and the masses were dried in desiccator, dried masses were crushed and pulverized. All

the dried SDs were passed through a sieve of 180 mm, kept in desiccators at room temperature until further analysis.

Solubility Studies

An excess quantity of SDs were taken in 25mL vial containing 10mL 0.1N HCl (pH 1.2) as a media. Then the samples were placed in thermostat shaking incubator (SI900R, Robus Technology, UAE) at 37±0.5°C for five days at 100 rpm. After five days, equilibrated samples were centrifuged at 600 rpm for 15 minutes and withdrawn by the use of syringe filter equipped with 0.45µm membrane filter. All the withdrawn samplers were analyzed spectrophotometrically (UV-1800, Shimadzu, Japan) at 242 nm in triplicates.

FTIR, PXRD, DSC and SEM

FTIR spectra of drug, polymers and formulations were obtained from ATR-FTIR 7600 spectrometer (Lambda, Australia) at 4000-450cm^{-1}. PXRD patterns of ZA, EPO, P188, P407 and SDs of binary and ternary systems were traced by X-Ray diffractometer, JDX-3532, JEOL, Japan with Cu-Kα radiation at 40kV and 30mA, measuring over a 2Θ range from 5 to 60 with scan step of .05° DSC analysis was performed on thermal analyzer (SDT Q600, V20.9 Build, TA instruments, USA) by heating the samples in an aluminum foil at the rate of 10°C/min under nitrogen gas flow to make the inert conditions.

SEM was performed to identify the surface topology and nature of pure ZA, EPO, P188, P407 and SDs. The SEM analysis was performed by scanning electron microscope (JSM, 6380L, JEOL/EO, Japan). Prior to observations, samples were placed on an aluminum stub by the use of double-sided adhesive tape and coated with a thin layer of gold (approximately 20 nm) in the vacuum. The operating acceleration voltage was 10 kV and observations were made at different magnifications and resolutions.

In vitro drug release studies and kinetic modeling

The *in vitro* dissolution studies of ZA and formulations were observed by utilizing USP dissolution apparatus II (Digitek, Lahore, Pakistan) with stirring speed of 50 rpm at 37±0.5°C in 900mL of freshly prepared 0.1N HCl having pH 1.2 as a dissolution medium. In the dissolution experiment, each sample was equivalent to 20 mg ZA. On specific time intervals such as 0, 2.5,5,10, 15, 30,45, 60, 90 and 120 minutes, aliquots of 5mL were taken out which were replaced through the addition of equal volume of fresh medium. These obtained samples were assayed at 242 nm, after filtration through 0.45 mm membrane filter. The dissolution data was analyzed using various kinetic models including zero order, first order, Higuchi and Korsemeyer-Peppas models. Korsmeyer-Peppas and Hixon Crowell model involve the fitting of initial 60% drug release data to find out the mode of drug release (Saeed *et al.*, 2019)

STATISTICAL ANALYSIS

GraphPad Prism 8 was utilized to calculate the mean and standard deviation.

RESULTS

Solubility Studies

Solubility studies were conducted in 0.1N HCl pH 1.2 to find out the changes in ZA solubility by binary SDs and ternary SDs. ZA is known to have poor aqueous solubility (Madsen *et al.*, 2016). The findings of the studies revealed that increments in solubility are dependent upon the concentration of the solubility enhancers (Saeed *et al.*, 2019). It was observed that SE technique was more efficient in achieving the task. Solubility of pure was 1.43±0.5µg/mL, but increased as the proportion of EPO (fig. 1) increased up to 1:7 ratio in PM, KM and SE based SD respectively (Mehmood *et al.*, 2019). SE9 was chosen for ternary SDs as it displayed highest solubility in binary SDs.

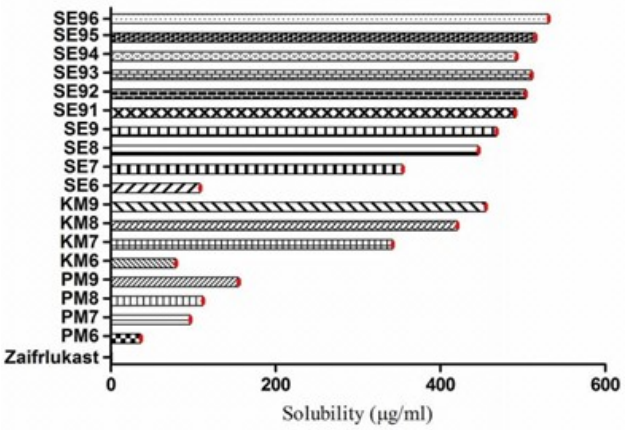

Fig. 1: Solubility of pure ZA and drug polymer complexes at 37°C in 0.1N HCl

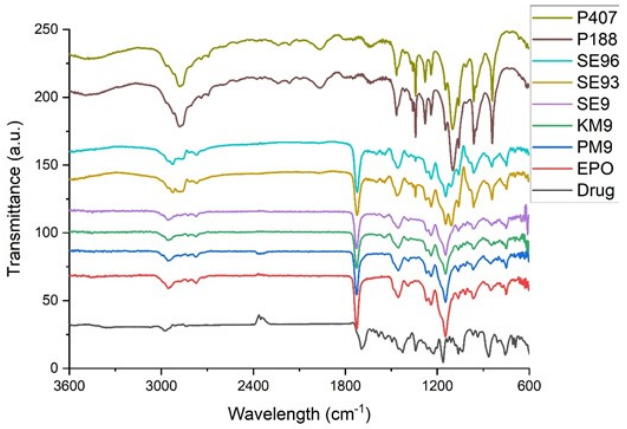

Fig. 2: FTIR spectra pure ZA and EPO, P188 and P407 formulations

FTIR, PXRD, DSC and SEM

FTIR has been employed most widely for identification of possible interactions among drug and polymers in

formulations. FTIR of ZA showed (fig. 2) the characteristic bands at 1693.1cm^{-1} (C=O stretching), 1538cm^{-1} (C=C stretching), 1340.2cm^{-1} (O=H bending), 1062.5cm^{-1} (C=O stretching), 1035.5cm^{-1} (C-O stretching) and 863.2cm^{-1} (=C-H bending). EPO showed strong bands for aldehyde at 1727.9cm^{-1} (C=O stretching) and ether at 1147.4 cm^{-1} (C-O-C asymmetric stretching (Alshehri *et al.*, 2017). P 188 and P407 showed bands at 2880.6 cm^{-1} (C-H stretching), 1466.6cm^{-1} (-CH_2 bending), 1341.73 cm^{-1} (C-H bending), 1279.2cm^{-1} (C-O stretching) and 1098.2cm^{-1} (C-O-C stretching) as mentioned elsewhere (Alshehri *et al.*, 2017, Mehmood *et al.*, 2019).

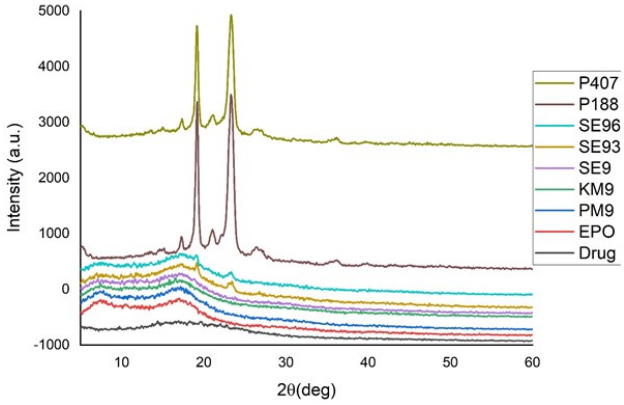

Fig. 3: PXRD spectra pure ZA and EPO, P188 and P407 formulations

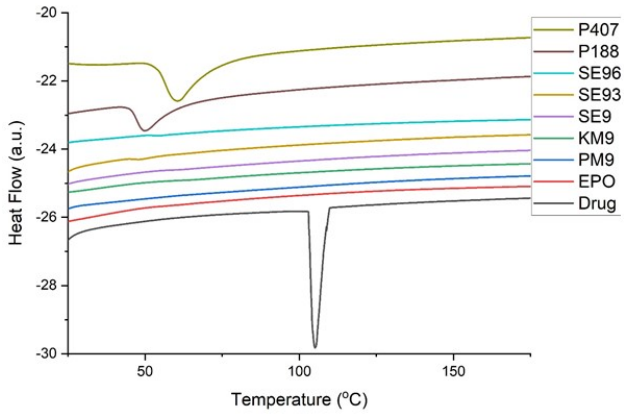

Fig. 4: DSC of pure ZA and EPO, P188 and P407 formulations

PXRD of ZA showed amorphous state of the active pharmaceutical ingredient (fig. 3). Due to amorphous physical texture, few distinct characteristics non intrinsic diffraction peaks appeared at a diffraction angle of 2Ɵ at 5.35, 9,75, 13.75, 14.4, 16.90, 18.35 and 19.60 (Thakral *et al.*, 2016). EPO exhibited amorphous physical texture with few non intrinsic peaks pattern with angle of diffraction at 7.05 and 17.05 (Feng *et al.*, 2019, Pradhan *et al.*, 2016). Both ternary polymers, P188 and P407, showed sharp intrinsic peaks with high intensity at diffraction angle between 18 to 23 (Kajdič *et al.*, 2018).

In DSC assessment (fig. 4), ZA thermogram revealed single endothermic event at 103^{O}C and our results conform well with the previously reported findings (Madsen *et al.*, 2016). The absence of peaks in SD is directly related with the concentration and interaction of polymers with ZA, as observed from FTIR and PXRD patterns.

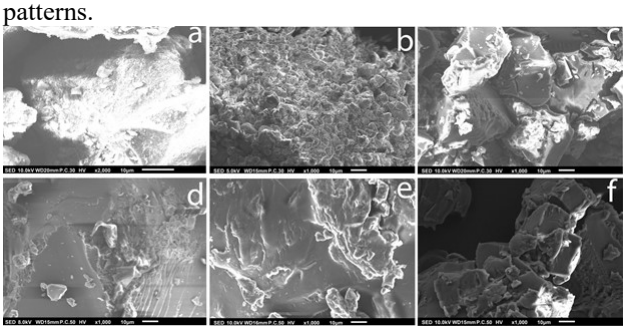

Fig. 5: SEM photographs of ZA (a), PM9 (b), KM9 (c), SE9 (d), SE93 (e), SE96 (f)

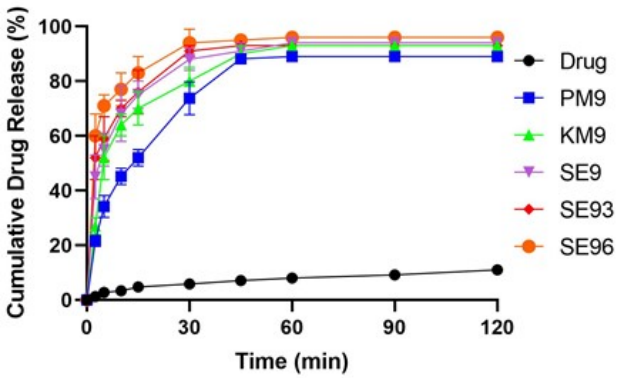

Fig. 6: *In-vitro* drug release behavior of pure ZA and formulations in 0.1 N HCl pH 1.2

Fig. 5 shows the SEM photomicrographs of drug, polymers and the SDs at selected magnifications. Pure ZA showed composite amorphous form (Huang and Williams, 2018). Binary dispersion with EPO and ternary dispersions withP188 and P407 showed smooth amorphous particulate forms (Mehmood *et al.*, 2019, Porfiryeva *et al.*, 2019) and P188 (Gajera *et al.*, 2016, Shi *et al.*, 2017).

ZA has very poor dissolution rate (<15% dissolved within 2 hours) in 0.1N HCl having pH 1.2. Rapid change in *in vitro* dissolution (>50%) was identified with EPO binary SD and ternary SDs with P188 and P407 in acidic environment within 10 minutes for all formulations (fig. 6). Whereas, SE93 and SE96 showed almost 90% drug release within 30 minutes. So, the higher percentage of P188 and P407 (10%) produced the maximum drug dissolution within shortest time.

DISCUSSION

ZA is an orally given leukotriene receptor antagonist employed in chronic asthmatics conditions (Yoon *et al.*,

Table 1: Drug-Polymer ratios of ZA with EPO, P188 and P407 for SD's

SD	Formulation	ZA	EPO	P188 (%)	P407 (%)
Binary	PM6	1	1	-	-
	PM7	1	3	-	-
	PM8	1	5	-	-
	PM9	1	7	-	-
	KM6	1	1	-	-
	KM7	1	3	-	-
	KM8	1	5	-	-
	KM9	1	7	-	-
	SE6	1	1	-	-
	SE7	1	3	-	-
	SE8	1	5	-	-
	SE9	1	7	-	-
Ternary	SE91	1	7	2.5	-
	SE92	1	7	5	-
	SE93	1	7	10	-
	SE94	1	7	-	2.5
	SE95	1	7	-	5
	SE96	1	7	-	10

Table 2: Statistical parameters of formulation fitting of drug release profile to various kinetic models

Kinetic Model		Zafirlukast	PM9	KM9	SE9	SE93	SE96
Zero Order	K_0	0.112543147	1.07	1.117579522	1.149777211	1.18	1.207985
	R^2	0.663234887	0.008538857	-0.732915684	-1.275522652	-1.5	-2.05566
1st Order	K_1	0.001201044	0.05229518	0.100972284	0.136971677	0.16	0.256083
	R^2	0.691503711	0.938093171	0.902077045	0.894526233	0.89	0.911864
Higuchi Model	K_H	1.042184266	10.43227131	11.18591385	11.63504192	12	12.39164
	R^2	0.986905058	0.798154771	0.494174585	0.258798632	0.15	-0.16128
Korsmeyer-Peppas	KP	1.262728645	23.58132647	36.912726	45.8515205	50.2	60.19384
	R^2	0.991293483	0.939114981	0.931609638	0.962410035	0.97	0.980314
	n	0.454	0.301871793	0.208	0.163	0.15	0.11
Hixson-Crowell	K_T	0.000391732	0.011458997	0.012501801	0.012868135	0.01	0.013369
	R^2	0.682262739	0.861092039	0.554452717	0.30984157	0.18	-0.17284

2018). Its poor aqueous solubility in body fluids is associated with poor bioavailability after an oral administration (Madsen *et al.*, 2016, Neeharika and Jyothi, 2021). Acetone was selected for dissolving ZA as it displayed highest drug solubilization capacity (Neeharika and Jyothi, 2021), whereas EPO, P188 and P407 were solubilized in methanol, that's why these solvents were used for the preparation of SDs by KM and SE.

From solubility studies, among all the binary SD formulations, SE9 was found optimal formulation with highest solubility 467±0.4µg/mL and was selected for ternary SDs (2.5%, 5% and 10% of total SD mass). Among ternary SD formulations, SE93 and SE96 showed maximal solubility increase of 510±0.48 and 531±0.63 µg/mL, respectively. SE96 (10% P407) showed maximum increase in overall solubility of almost 356 folds. Whereas, least solubility improvement was observed for PM9 (fig. 1).

It was clear from comparison of FTIR spectra that ZA's maintained its chemical integrity in all the formulations, but physical interactions increased with the increase in polymers concentrations in binary and ternary systems. Most of the peaks of ZA were absent in binary systems indicating drug trapping and complexation with the polymer. Similarly, ternary formulations displayed peaks of both polymers. Slight band shifts towards lower wavelengths were observed. This study is in good agreement with the previously reported performance of polymers (Alshehri *et al.*, 2017, Yadav and Tanwar, 2016) that increasing the concentration of polymers leads to diminishing of the peaks of drugs due to physical interactions, hydrogen bonding and van der waal's attractions (Mehmood *et al.*, 2019, Saeed *et al.*, 2019).

PXRD results confirm the perseverance of the amorphousness of ZA in binary and ternary systems (Kajdič *et al.*, 2018, Sheng *et al.*, 2018). In DSC thermograms, no peak of ZA was detected in the

formulation of binary and ternary systems. This absence of peak indicates the ZA interacted with the polymers at molecular level and got entrapped in the polymeric matrices of both binary and ternary systems. Drug's glass transition temperature disappeared in formulations further complimenting the observations of massive increase in solubility. Surface morphology of binary and ternary systems support the increased amorphousness of drug composites. No phase separation was observed and the resultant formulations appear as homogenized systems.

Dissolution rate of pure ZA over a time duration of 2 hours was very low (11.4%). In binary SDs, PM9 showed 52 % release in 15 minutes, whereas at same time span, KM9 and SE9 showed 70.8% and 75.2%, respectively. A maximum of 91.42% and 94.2% drug release within 30 minutes was observed for SE93 and SE96, respectively. So, the highest and optimal drug release improvement was observed for SE96 made up of P407, which was 8.3 folds higher than the pure ZA after 2 hours. Statistical parameters drug release profile to various kinetic models revealed that pure drug dissolution was a zero-order process, whereas, all the SDs followed the 1st order drug release kinetics. Value of n of Korsmeyer-Peppas model was below 1 for the SDs that confirms the 1st order release behavior by diffusion.

CONCLUSION

The present study reveals the capability of the EPO to boost the solubility of ZA by solvent evaporation technique, which is further strengthened by the incorporation of P188 or P407. Characterizations of formulations by FTIR, DSC, SEM and PXRD indicate the formation of stable binary and ternary systems with optimum behavior. Use of P407 as the ternary component was singled out as the best approach to develop the SD of ZA with EPO for maximum solubilization and dissolution of ZA.

REFERENCES

Agafonov M, Volkova T, Kumeev R, Chibunova E and Terekhova I (2019). Impact of pluronic F127 on aqueous solubility and membrane permeability of antirheumatic compounds of different structure and polarity. *J. Mol. Liq.*, **274**: 770-777.

Alshehri S, Shakeel F, Ibrahim M, Elzayat E, Altamimi M, Shazly G, Mohsin K, Alkholief M, Alsulays B and Alshetaili A (2017). Influence of the microwave technology on solid dispersions of mefenamic acid and flufenamic acid. *PloS One*, **12**(7): e0182011.

Barkat MA, Rizwanullah M, Beg S, Pottoo FH, Siddiqui S and Ahmad FJ (2019). Paclitaxel-loaded nanolipidic carriers with improved oral bioavailability and anticancer activity against human liver carcinoma. *AAPS PharmSciTech*, **20**(2): 1-14.

Delijewski M and Haneczok J (2021). AI drug discovery screening for COVID-19 reveals zafirlukast as a repurposing candidate. *Med. Drug Discov.*, **9**: 100077.

Drašković M, Medarević D, Aleksić I and Parojčić J (2017). In vitro and in vivo investigation of taste-masking effectiveness of Eudragit E PO as drug particle coating agent in orally disintegrating tablets. *Drug Dev. Ind. Pharm.*, **43**(5): 723-731.

Feng Z, Li M and Wang W (2019). Improvement of dissolution and tabletability of carbamazepine solid dispersions with high drug loading prepared by hot-melt extrusion. *Pharmazie*, **74**(9): 523-528.

Gajera BY, Dugar RP and Dave RH (2016). Formulation development and optimization of ibuprofen poloxamer melt granules using hydrophilic excipients. *J. Pharm. Res. Int.*, **13**(6): 1-19.

Huang S and Williams RO (2018). Effects of the preparation process on the properties of amorphous solid dispersions. *AAPS PharmSciTech*, **19**(5): 1971-1984.

Kajdič S, Vrečer F and Kocbek P (2018). Preparation of poloxamer-based nanofibers for enhanced dissolution of carvedilol. *Eur. J. Pharm. Sci.*, **117**: 331-340.

Kumar P, Agarwal A, Singh AK, Gautam AK, Chakraborti S, Kumar U, Kumar D, Bhattacharya B, Panda P and Saha B (2019). Antineoplastic properties of zafirlukast against hepatocellular carcinoma via activation of mitochondrial mediated apoptosis. *Regul. Toxicol. Pharmacol.*, **109**: 104489.

Lei C, Wu S, Wen C, Li Y, Liu N, Huang J, Li L, Fu M and Liu J (2019). Zafirlukast attenuates advanced glycation end-products (AGEs)-induced degradation of articular extracellular matrix (ECM). *Int. Immunopharmacol.*, **68**: 68-73.

Madsen CM, Boyd B, Rades T and Müllertz A (2016). Supersaturation of zafirlukast in fasted and fed state intestinal media with and without precipitation inhibitors. *Eur. J. Pharm. Sci.*, **91**: 31-39.

McPherson S, Perrier J, Dunn C, Khadra I, Davidson S, Ainousah B, Wilson CG and Halbert G (2020). Small scale design of experiment investigation of equilibrium solubility in simulated fasted and fed intestinal fluid. *Eur. J. Pharm. Biopharm.*, **150**: 14-23.

Mehmood HQ, Faran SA, Chaudhry MA, Khalid SH, Khan IU, Hassan W, Ashfaq R and Asghar S (2019). An assessment of bioavailability of acrylate based pH-sensitive complexes of lovastatin. *Pak. J. Pharm. Sci.*, **32**(3 (Suppl)): 1129-1136.

Nanaki S, Eleftheriou RM, Barmpalexis P, Kostoglou M, Karavas E and Bikiaris D (2019). Evaluation of dissolution enhancement of aprepitant drug in ternary pharmaceutical solid dispersions with Soluplus® and Poloxamer 188 prepared by melt mixing. *Sci*, 1(2): 48.

Neeharika M and Jyothi BJ (2021). Preparation and Evaluation of Zafirlukast Compression Coated Tablets for Chronotherapeutic Drug Delivery. *J. Pharm. Res. Int.*, **33**(32B): 154-166.

Porfiryeva NN, Nasibullin SF, Abdullina SG, Tukhbatullina IK, Moustafine RI and Khutoryanskiy VV (2019). Acrylated Eudragit® E PO as a novel polymeric excipient with enhanced mucoadhesive properties for application in nasal drug delivery. *Int. J. Pharm.*, **562**: 241-248.

Pradhan R, Kim SY, Yong CS and Kim JO (2016). Preparation and characterization of spray-dried valsartan-loaded Eudragit® E PO solid dispersion microparticles. *Asian J. Pharm. Sci.*, **11**(6): 744-750.

Rajasekhar D, Srinivasulu D, Sridhar C, Kumar GVN and Ramesh P (2016). Synthesis, Spectral Characterization and Antioxidant Activity of Novel Zafirlukast Sulfonyl Derivatives. *J. Chin. Chem. Soc.*, **63**(3): 267-274.

Saeed MA, Ansari MT and Ch BA (2019). Enhancement of solubility and dissolution profile of artesunate by employing solid dispersion approach: An in-vitro evaluation. *Pak. J. Pharm. Sci.*, **36**(1 (Suppl)): 353-361.

Schierle S, Flauaus C, Heitel P, Willems S, Schmidt J, Kaiser A, Weizel L, Goebel T, Kahnt AS and Geisslinger G (2018). Boosting anti-inflammatory potency of zafirlukast by designed polypharmacology. *J. Med. Chem.*, **61**(13): 5758-5764.

Sheng X, Tang J, Bao J, Shi X and Su W (2018). Enhancement of in vitro dissolution and in vivo performance/oral absorption of FEB-poloxamer-TPGS solid dispersion. *J. Drug Deliv. Sci. Technol.*, **46**: 408-415.

Shi N-Q, Zhang Y, Li Y, Lai H-W, Xiao X, Feng B and Qi X-R (2017). Self-micellizing solid dispersions enhance the properties and therapeutic potential of fenofibrate: Advantages, profiles and mechanisms. *Int. J. Pharm.*, **528**(1-2): 563-577.

Song Q, Hu Z, Xie X and Cai H (2020). Zafirlukast prevented ox-LDL-induced formation of foam cells. *Toxicol. Appl. Pharmacol.*, **409**: 115295.

Tambe A and Pandita N (2018). Enhanced solubility and drug release profile of boswellic acid using a poloxamer-based solid dispersion technique. *J. Drug Deliv. Sci. Technol.*, **44**: 172-180.

Thakral S, Terban MW, Thakral NK and Suryanarayanan R (2016). Recent advances in the characterization of amorphous pharmaceuticals by X-ray diffractometry. *Adv. Drug Deliv. Rev.*, **100**: 183-193.

Yadav B and Tanwar Y (2016). Development, characterization and in vitro evaluation of flurbiprofen solid dispersions using polyethylene glycols as carrier. *J. App. Pharm. Sci.*, **6**(04): 060-066.

Yang L, Chen X, Ni K, Li Y, Wu J, Chen W, Ji Y, Feng L, Li F and Chen D (2020). Proton-exchanged montmorillonite-mediated reactions of hetero-benzyl acetates: Application to the synthesis of Zafirlukast. *Tetrahedron Lett.*, **61**(29): 152123.

Yoon I, Han H and Kim J (2018). Successful management of refractory cough with the leukotriene receptor antagonist zafirlukast in a dog with chronic bronchitis: a case report. *Vet. Med.*, **63**(4): 181-186.

Zeng C, Wang D, Chen C, Chen L, Chen B, Li L, Chen M and Xing H (2020). Zafirlukast protects blood-brain barrier integrity from ischemic brain injury. *Chem. Biol. Interact.*, **316**: 108915.